

Design of Spacecraft Swarm Flybys for Planetary Moon Exploration

Ravi teja Nallapu* and Jekanthan Thangavelautham.†
University of Arizona, Tucson, AZ-85719.

Exploration of small bodies brings insight to the origins of the life, the Earth, and the solar system. However, attempting surface missions to small-bodies with inadequate gravity field information is prone to high-risk of failure. Spacecraft flybys can be a viable approach to perform an initial reconnaissance before a surface mission can be deployed. The challenge with flybys is that they are time and coverage limited thus providing only a limited glimpse of the target. These disadvantages can be overcome using a swarm approach. While swarms are important platforms for small-body exploration, their mission design is a complex design problem, and more importantly, there is no end-to-end tool for designing spacecraft swarm missions. This paper presents IDEAS, an end-to-end mission design architecture that designs swarm missions for small body flyby exploration. The IDEAS platform, at its heart, will have three automated design modules corresponding to spacecraft design, swarm design, and trajectory design. In our previous work, we developed the Automated Swarm Designer module of the IDEAS platform to explore uniformly rotating asteroids. The current work will focus on enabling the IDEAS architecture to design visual mapping missions to planetary moons through spacecraft swarm flybys. Specifically, a swarm of spacecraft will be designed to explore a target moon through multiple encounters at different orbital locations using hyperbolic trajectories around the central planet. The objective of the designed swarm is to produce a detailed surface map of the moon with a minimum number of spacecraft. Here, we show that the design of swarm trajectories will result in a boundary value problem, where we have a rendezvous location and an excess velocity asymptote. This boundary value problem will be formulated as a system of non-linear equations which will then be solved using an iterative scheme. The solutions to this will specify a hyperbolic reconnaissance trajectory of a participating spacecraft in the swarm. We then determine the optimal set of these flyby trajectories using an evolutionary search algorithm to meet the required coverage criterion with a minimum number of spacecraft. Finally, the algorithms developed in this work are demonstrated through a theoretical example of designing a reconnaissance mission to the Martian moon Phobos.

I. Introduction

PLANETARY moons are high priority science targets. In situ missions to their surface will help to achieve major scientific goals set out in the recent planetary science decadal survey [1, 2]. In addition, more practical studies to use these moons to facilitate interplanetary travel have also been made [3]. However, the dynamical and physical environment around these moons offer a lot of uncertainty which can be high-risk for in-situ mission [4, 5] unless detailed reconnaissance is done beforehand. While such reconnaissance can be done using orbits, the micro-gravity environment is often a challenge for the orbital stability [6], and more importantly, these orbiter missions have to account for an insertion maneuver which can be expensive in terms of fuel. Flybys utilizing hyperbolic trajectories offer a potential solution for small body reconnaissance. Planetary moon flybys have been a major source of human understanding of the planetary moons. Historical flybys of the Pioneer [7] and Voyager missions [8] have immensely contributed to the knowledge of the moons of outer planets such as Jupiter and Saturn. The flyby trajectories of two Voyager spacecraft near Saturn and their photo contributions of the Saturnian moons are presented in Figure 1.

However, flyby missions are limited by their spatial and temporal coverage. Furthermore, this coverage is constrained by self-shadowing, which limits the amount of illuminated surface to around 50 %. While these challenges are complex to be solved by a single spacecraft, they can be well handled by a swarm of multiple spacecraft. Design of a swarm mission is a multi-disciplinary problem as it involves the selection of several system-level parameters such as the number

*Ph.D. Candidate, Aerospace Engineering, rnallapu@email.arizona.edu

†Assistant Professor, Aerospace and Mechanical Engineering Department, jekan@email.arizona.edu

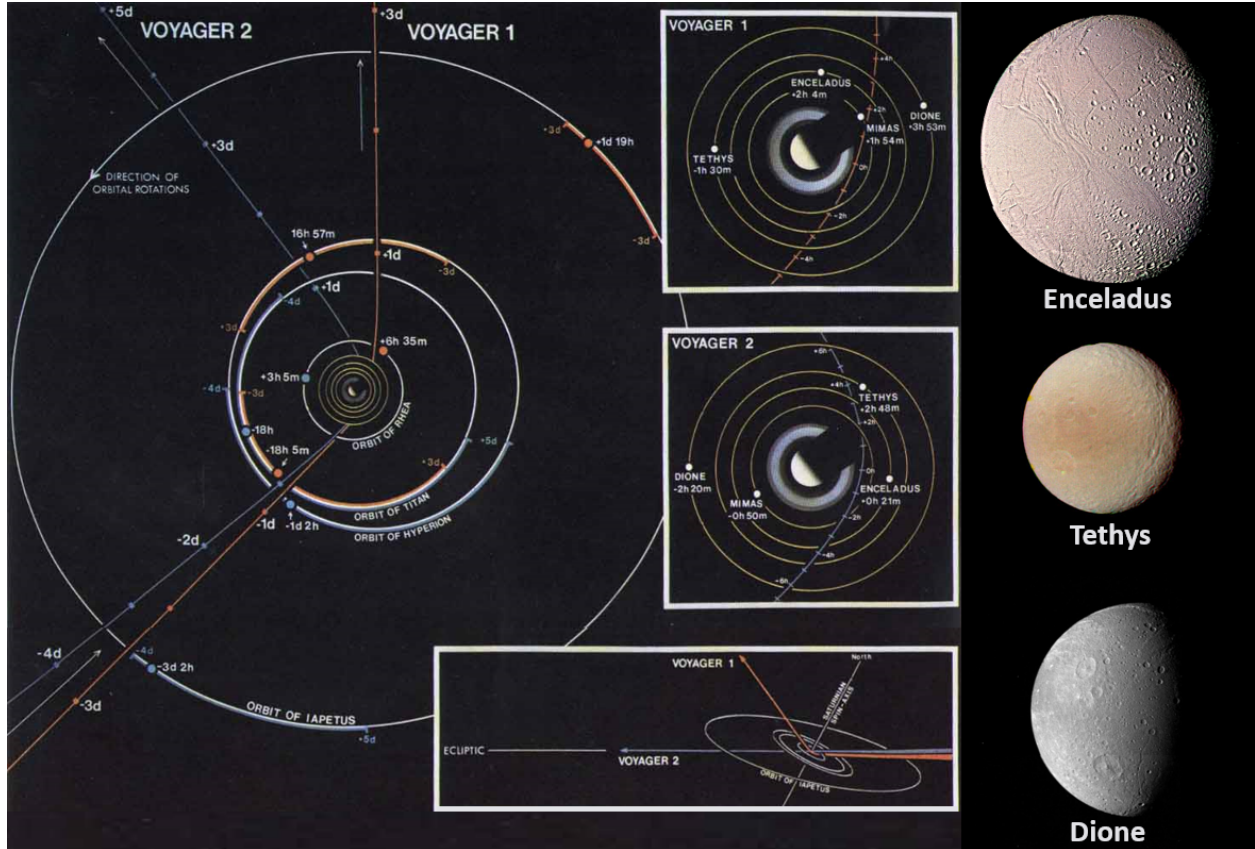


Fig. 1 The flyby trajectories of the two Voyager spacecraft around Saturn (left), and the images of the planetary moons taken during these flybys (right). [Image credit: NASA]

of spacecraft, choice of payload, and other subsystems, etc. These designs can greatly benefit from an end-to-end swarm mission design tool. To address these challenges, we developed the Integrated Design Engineering and Automation of Swarms (IDEAS), a mission architecture to design interplanetary swarm missions [9]. In the IDEAS framework, a swarm mission design is handled by three automated design modules trajectory, swarm, and spacecraft as shown in Figure 2. Each of these modules tries to optimize their respective objectives, and the collective validity of the design is checked by the Mission Analyzer module. In the current work, we explore the capability of the Automated Swarm Designer module of IDEAS to design swarm flyby missions that generate global surface maps of planetary moons. The swarms will be designed to be in hyperbolic trajectories with respect to the central planet around the moon. Due to the high energy nature of the hyperbolic trajectories, the gravitational effects of the moon will be assumed to be negligible.

We begin by presenting a new design methodology to shape the encounter of the swarm. The method involves selecting a point on the encounter trajectory with respect to the moon, which is capable of making the desired observation. This coupled with the incoming excess velocity asymptote, \hat{V}_{∞}^- can be used to define a hyperbolic trajectory of the spacecraft. In this work, we show that this boundary value problem will result in a system of non-linear equations, which will be solved using an iterative root-finding scheme. The trajectories will then be optimized to get the required coverage with a minimum number of spacecraft. Finally, the algorithms presented in this work will be demonstrated using a theoretical mission design to explore the Martian moon Phobos.

The organization of the current work is as follows: Section II presents related work done in the field of spacecraft swarms. Section III presents the methodology of the current work. Here we present the moon mapping design problem. The boundary value problem corresponding to the computation of the hyperbolic trajectories will also be formulated here. Section IV will demonstrate the capabilities of the algorithms presented to design a surface mapping mission to the Martian moon Phobos. Section V will identify and highlight the important contributions of the current work. Finally, Section VI will conclude the current work by providing a brief summary of the work followed by identifying

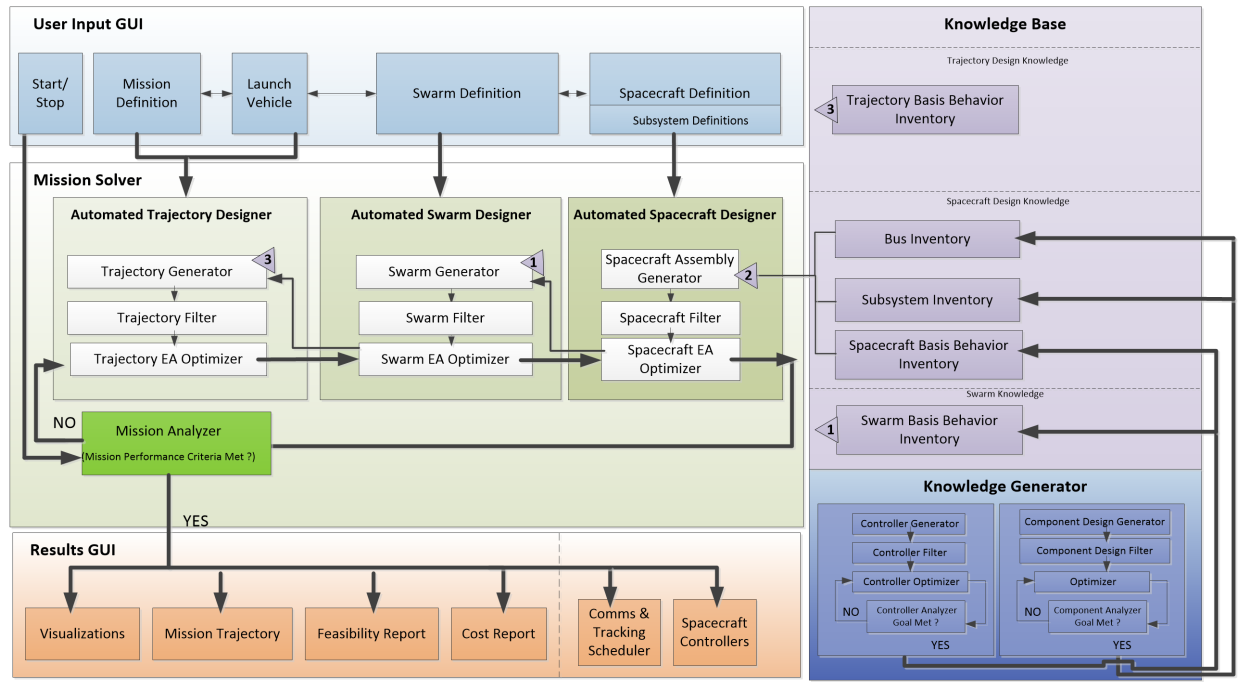


Fig. 2 Architecture of the IDEAS software for designing spacecraft swarm missions to small bodies.

pathways forward.

II. Related Work

Historically, spacecraft flybys have been the dominant method of exploring solar system small bodies. The Vega missions that explored the comet 1P/Halley through flybys [10] are amongst the first small body exploration missions in human history. Several prominent missions such as Giotto [11], Sakigake [12], International Comet Explorer (ICE) [13], Stardust [14], Deep Impact [15], have relied on flyby trajectories to make their observation. More relevant to the current topic, the Pioneer [7] and the Voyager [8] missions have led to some of the first observations of the moons of Jupiter and Saturn. The flyby trajectory design problem for moon exploration is mainly posed as a timing problem. In this case, the spacecraft trajectory closely passes the orbit of the moon, when resolved in an inertial reference frame of the central planet. The spacecraft is then phased on its trajectory such that the moon and the spacecraft will be close enough during the spacecraft arrival. These strategies only allow a limited glimpse of the target moon. A new design strategy is required if we are interested in generating global surface maps of the target bodies through spacecraft flybys. Furthermore, since such swarm designs are influenced by spacecraft design, and the interplanetary trajectory design. For this reason, a unifying mission design scheme where the spacecraft, trajectories, and the swarm are designed simultaneously can result in holistically optimal designs that are often intuitive to traditional mission design methods [16]. In order to address these challenges, we developed the Integrated Design Engineering and Automation of Swarms (IDEAS) for the automated design of such spacecraft swarm missions [9]. Following this, we applied developed the capability of IDEAS for different mission design applications. In our previous work, we designed visual mapping missions to uniformly rotating asteroids [9, 17]. We have also applied the IDEAS methodology to design Earth monitoring constellations [18, 19], and constellations to enable communications in the cislunar space [20]. Our previous work also explored the design of a planetary moon mapping swarm, where the spacecraft in the swarm enter into an orbit around the central planet [21]. The current work will aim to enable swarm designs that explore planetary moons while remaining on hyperbolic trajectories around the central planet, thus avoiding orbit insertion maneuvers.

III. Methodology

We begin by introducing formulating a swarm flyby mapping mission as an optimization problem, along with the design gene. We then proceed to construct the hyperbolic trajectories from a given design gene. As mentioned above, the trajectories will be constructed by solving a system of nonlinear equations.

A. Mapping Mission

The objective of a moon mapping mission would be to generate global surface maps of the moon with a tolerance of ϵ_{map} . The observations will have a ground resolution constraint of x_D , and a minimum elevation angle of ϵ_D . This allows us to estimate the altitude required h_f for imaging the moon as:

$$h_f = \frac{x_D D_C}{\lambda_D} \quad (1)$$

Where D_C is the aperture diameter of the spacecraft camera, and λ_D is the wavelength of the imaging sensor. The red spectrum can be taken as a baseline for this purpose since it guarantees that the entire visual spectrum is imaged. Similarly, the required half field of view spacecraft η_D is given by

$$\sin \eta_D = \left(\frac{R_T}{R_T + h_f} \right) \cos \epsilon_D \quad (2)$$

Where R_T is the average radius of the target moon. Finally, the mission design altitude for the mission can be selected as

$$h'_f = h_f - \Delta h \quad (3)$$

Where Δh is a user-specified tolerance parameter.

B. Trajectory Design

The trajectory design addresses the launch of spacecraft from the Earth, and arrival at the target planet. We assume that the complete swarm is launched from Earth on the same launch date D_L and arrives in the neighborhood of a selected arrival date D_A . The launch and arrival dates can be used to define a heliocentric Lambert arc between the launch and arrival planets. The Lambert arc provides the excess velocity asymptotes at the launch $\bar{V}_{\infty,1}^+$ and arrival $\bar{V}_{\infty,2}^-$. The mission-critical parameters like launch energy (C_3), time of flight (ToF), and excess velocity magnitude at arrival $v_{\infty,2}^-$ can be easily extracted from these asymptotes [22]. Since the encounter velocities with the target moon are directly related to the excess velocities of the spacecraft at the arrival planet, the ease of imaging could be improved by selecting trajectories with low $v_{\infty,2}^-$. Additionally, the trajectories selected should have practical bounds on the launch energy $C_{3,max}$, and time of flight ToF_{max} . Additionally, the right ascension RAA , and declination DAA of the arrival asymptote can also be extracted from $\bar{V}_{\infty,2}^-$, which will be used to construct the swarm trajectories. The automated trajectory design problem then is a search for launch and arrival dates which produces a feasible trajectory with the least excess velocity at arrival, posed as

$$\begin{aligned} \min \quad & J_T = v_{\infty,2}^- \\ \text{s.t.} \quad & D_{L,min} \leq D_L \leq D_{L,max} \\ & D_{A,min} \leq D_A \leq D_{A,max} \\ & C_3 \leq C_{3,max} \\ & ToF \leq ToF_{max} \end{aligned} \quad (4)$$

Where the bounds on launch and arrival dates are defined by the user. The design gene of the automated trajectory design problem is shown in Figure 3.

Parameter	Launch date	Arrival date
Variable	D_L	D_A
Range	Integer $[D_{L,min}, D_{L,max}]$	Integer $[D_{A,min}, D_{A,max}]$

Fig. 3 Gene map of the trajectory design problems showing different design variables and their attributes.

C. Swarm Configuration

We assume that a spacecraft swarm will continuously image the target moon once their altitude with respect to the target falls below the required imaging altitude in Equation 1. Let us assume that during a single pass, a swarm of N_j spacecraft will pass by the moon at an altitude h'_f . In order to shape the encounter of the swarm, we allow the spacecraft i in the swarm to perform a flyby of the moon at right ascension $\theta_{x,i}$, and declination $\theta_{y,i}$ as shown in Figure 4. If the surface of the moon is completely illuminated, a single pass of the moon is sufficient to generate a global surface map. However, since at any given time, roughly 50% of the moon is in the hard shadow of the Sun, we allow the swarm to generate the global map N_v passes. Furthermore, to generalize these designs, we allow each visit to have $N_{v,j}$ spacecraft, where j is the index corresponding to the pass number. The visiting location of the moon is characterized by its true anomaly $f_{v,j}$. The swarm size can now be computed as

$$N_{Sw} = \sum_{j=1}^{N_v} N_{v,j} \quad (5)$$

This allows us to categorize the design parameters as orbital parameters, and encounter shaping parameters as shown in Figure 4. The visual surface coverage P_{cov} capable by a given swarm can be computed, if the shape model of the moon is available, using the algorithms described in [9]. Additionally, we assume that the current spacecraft swarm has the same Class 2 architecture as describes in [17], which suggests that the observing spacecraft coordinate with a leader spacecraft for communication.

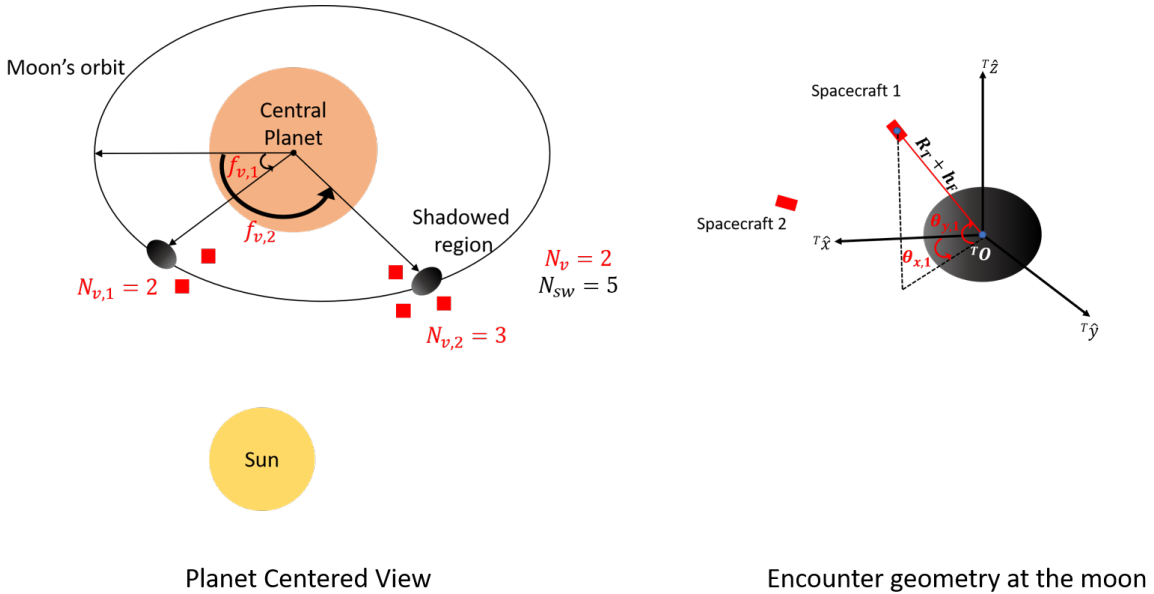


Fig. 4 Spacecraft swarm configuration showing the orbital design parameters (left) and encounter shaping parameters (right).

D. Flyby Trajectory Construction

The previous sections described the interplanetary trajectory of the swarm, and how their encounters are shaped with respect to the moon. Here we describe an algorithm that ensures that the encounter trajectories can be accomplished with the designed interplanetary trajectory. More specifically, we ensure that the encounters share the same incoming hyperbolic asymptote as shown in Figure 5. As described above, selecting the visiting altitude h'_f , and the right ascension $\theta_{x,i}$, and declination angles $\theta_{y,i}$, allow us to compute a position vector of spacecraft i in a moon centered inertial frame $\bar{r}_{i,SM}$ using a spherical coordinate to Cartesian transformation. The inertial location of the moon $\bar{r}_{j,MP}$ at a true anomaly $f_{v,j}$, can be computed by transforming the orbital elements to Cartesian coordinates. The vector sum of $\bar{r}_{i,SM}$ and $\bar{r}_{j,MP}$ allows us to determine the inertial location of spacecraft i with respect to the central planet $\bar{r}_{i,SP}$ as

$$\bar{r}_{i,SP} = \bar{r}_{i,SM} + \bar{r}_{j,MP} \quad (6)$$

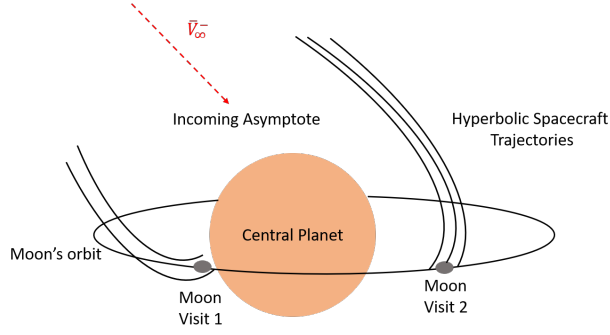


Fig. 5 The design condition on the hyperbolic trajectories stating that all encounters should share the same incoming asymptote.

In order to propagate the trajectory forward, we need the complete spacecraft state (position, and velocity) at an instant in time. However, the current problem defines the position vector of the spacecraft at one instant, and the excess velocity vector of the incoming asymptote at another. Therefore, propagating the flyby trajectories turns into a boundary value problem. In order to solve this problem, we compute the planet centered velocity vector at the time of encounter. Let $\bar{V}_{i,SP} = [v_x \ v_y \ v_z]^T$ be this unknown velocity vector. The vis viva equation [22] allows us to constrain this velocity vector as

$$|\bar{V}_{i,SP}|^2 = v_x^2 + v_y^2 + v_z^2 = \left(v_{\infty,2}^-\right)^2 + \left(\frac{2\mu_P}{r_{i,SP}}\right) \quad (7)$$

Where, μ_P is the gravitational parameter of the planet, and $r_{i,SP}$ is the magnitude of \bar{r}_i . In order to place additional constraints the orbital elements of the trajectory will be computed. The semi-major axis a can be easily determined from $v_{2,\infty}^-$ [22]. The eccentricity vector is written as

$$\bar{e}_i = \frac{1}{\mu_P} \left(\left(v_{i,SP}^2 - \left(\frac{\mu_P}{r_{i,SP}} \right) \right) \bar{r}_{i,SP} - (\bar{r}_{i,SP} \cdot \bar{V}_{i,SP}) \bar{V}_{i,SP} \right) \quad (8)$$

The specific angular momentum \bar{h}_i , and normal vector \hat{n}_i can be expressed as

$$\bar{h}_i = \bar{r}_{i,SP} \times \bar{V}_{i,SP} \quad (9)$$

and

$$\hat{n}_i = \hat{k} \times \frac{\bar{h}_i}{|\bar{h}_i|} = \hat{k} \times \bar{h}_i \quad (10)$$

Where, $\hat{k} = [0 \ 0 \ 1]^T$ is the z axis of the central planet's inertial frame. It should be noted here that the vectors expressed in Equations 8-10 are functions of the unknown velocity components. These can be used to define the orientation elements of the orbit. The right ascension Ω_i , inclination in_i , and argument of periapsis $\omega_{p,i}$ of the spacecraft can be determined as

$$\Omega_i = \begin{cases} \arccos\left(\frac{\hat{n}_{i,S}[1]}{|\hat{n}_{i,S}|}\right) & \hat{n}_{i,S}[1] \geq 0 \\ 2\pi - \arccos\left(\frac{\hat{n}_{i,S}[1]}{|\hat{n}_{i,S}|}\right) & \hat{n}_{i,S}[1] < 0 \end{cases} \quad (11)$$

$$in_i = \arccos\left(\frac{\hat{h}_i[3]}{|\hat{h}_i|}\right) \quad (12)$$

and

$$\omega_{p,i} = \begin{cases} \arccos(\hat{n}_i \cdot \hat{e}_i) & \hat{e}_i[3] \geq 0 \\ 2\pi - \arccos(\hat{n}_i \cdot \hat{e}_i) & \hat{e}_i[3] < 0 \end{cases} \quad (13)$$

Finally, the hyperbolic true anomaly $f_{\infty,i}$ is computed as

$$f_{\infty,i} = \arccos\left(\frac{-1}{e_i}\right) \quad (14)$$

Where the numbers inside [] indicate the component of the corresponding vector. On the entering asymptote, we set the true anomaly of the as $f_i = -f_{\infty,i}$. We can now write the asymptotic excess velocity vector

$$\bar{V}_{\infty,i} = \sqrt{\frac{\mu_P}{a(1-e_i^2)}} R_3(\Omega_i) R_1(in_i) R_3(\omega_{p,i}) \begin{bmatrix} -\sin(f_{\infty,i}) \\ e_i + \cos(f_{\infty,i}) \\ 0 \end{bmatrix} \quad (15)$$

Where R_1 and R_3 are principal rotation matrices about axes 1 and 3 respectively [23]. The right ascension RAA_i and declination DAA_i of spacecraft i can now be extracted from the asymptote as

$$RAA_i = \arctan\left(\frac{\bar{V}_{\infty,i}[2]}{\bar{V}_{\infty,i}[1]}\right) \quad (16)$$

and

$$DAA_i = \arcsin\left(\frac{\bar{V}_{\infty,i}[3]}{|\bar{V}_{\infty,i}|}\right) \quad (17)$$

This allows us to place final constraints on the trajectories as

$$RAA_i = RAA \quad (18)$$

and

$$DAA_i = DAA \quad (19)$$

for all spacecraft in the swarm. This ensures that all spacecraft share the same arrival asymptote. It should be noted here that Equations 7, 18, and 19 are nonlinear functions of the spacecraft velocity components, and should be solved using a nonlinear solvers. Typically, all root solvers require an initial guess. Through experimentation, we found that the velocity of the moon during the encounter, if used as an initial guess, produces faster convergences to the solutions. In this way, we can specify an encounter hyperbola by specifying an encounter point on its trajectory, and the arrival asymptote at the central planet.

E. Swarm Design

We can now pose the automated spacecraft swarm design problem as an optimization problem, where we are interested in determining the trajectories of the swarm which can meet a coverage requirement $P_{Cov,R}$ with a minimum number of spacecraft. Additionally, planetary periapsis altitude, and collision avoidance constraints as described in [21] can also be placed on the swarm. Therefore, the swarm design problem can be posed as

$$\begin{aligned}
 \min \quad & J_{Sw} = N_{Sw} \\
 \text{s.t.} \quad & P_{Cov} \geq P_{Cov,R} \\
 & h_{i,p} \geq h_p \quad \forall i \leq N_{Sw} \\
 & Collisions = False
 \end{aligned} \tag{20}$$

Where, h_p , and $h_{p,R}$ denote the planetary periapsis of the trajectory, and its corresponding user defined requirement respectively. The design variables of the swarm optimization problem are presented in Figure 6.

Parameter	# spacecraft visits	# Spacecraft each visit		True anomaly of the moon		Spacecraft RA at visit		Spacecraft Dec at visit					
Variable	N_v	$N_{v,1}$...	N_{v,N_v}	$f_{v,1}$...	f_{v,N_v}	$\theta_{x,1}$...	$\theta_{x,N_{Sw}}$	$\theta_{y,1}$...	$\theta_{y,N_{Sw}}$
Range	Integer [1, $N_{1,max}$]	Integer [1, $N_{2,max}$]		Real [0, 2π]		Real [0, 2π]		Real [$-\frac{\pi}{2}, \frac{\pi}{2}$]					

Fig. 6 Gene map of the swarm design problems showing different design variables and their attributes.

IV. Numerical Simulations

In this section, we demonstrate the results of the algorithms discussed here to design a spacecraft swarm mission to map the surface of the Martian moon Phobos. The objective of the notional mission can be stated as follows. We are interested in designing a swarm mission to generate at least 85% global surface maps of Phobos with a maximum ground resolution of 1 m, and a minimum elevation angle of 5 deg. A 32k triangular face shape model (see Figure 11) is used to model the surface of Phobos and its physical orbital characteristics [24].

A. Spacecraft Design

We assume that the spacecraft in the swarm have a CubeSat grade camera [25] with an aperture diameter of 8 cm. The flyby altitude and spacecraft field of view required are computed using Equations 1 and 2 as 114 km and 10.1 deg respectively. With a 5 km tolerance, the designed flyby encounter altitude is selected as 109 km.

B. Trajectory Design

The interplanetary trajectories of the swarm are obtained by solving Equation 4. The launch and arrival dates are obtained by constrained optimal search using a genetic algorithm optimizer. The user defined inputs to the trajectory design problem are presented in Table 1.

Table 1 User defined inputs and bounds supplied for the trajectory design problem.

Parameter	Value
Launch date range	Jan 1 st to Dec 31 st , 2020
Arrival date range	May 1 st , 2020 to Dec 31 st , 2020
Max C_3 energy	20 km ² /s ²
Max time of Flight	200 days

The genetic algorithm converged to an optimal solution within 5 generations, where it explored 7200 trajectories. The optimal trajectory of the swarm is presented in Figure 7. The pork chop plot was generated by solving Lambert's problem over a smooth grid of launch and arrival dates, by using a fast Lambert solver algorithm [26] developed at the

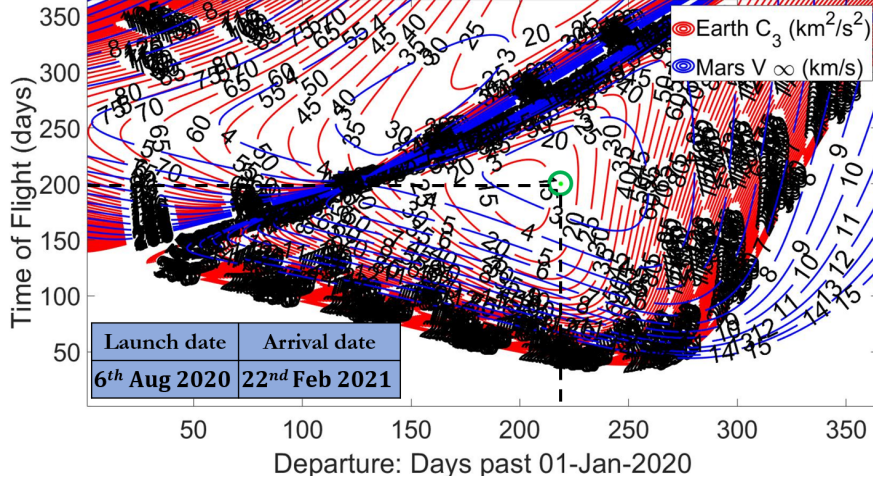


Fig. 7 The selected optimal solution of the trajectory design problem along with the Earth-Mars pork chop plot.

University of Texas. As seen in Figure 7, the optimal launch and arrival dates for the swarm are 6th August 2020 and 22nd August 2021 respectively. The trajectory would be launched with a C_3 energy of $16.6 \text{ km}^2/\text{s}^2$, and a time of flight of 200 days. The trajectory has a excess asymptotic velocity of 2.5 km/s at Mars. The RAA and DAA of the trajectory at arrival 29.1 deg and -14 deg respectively.

C. Swarm Design

The automated swarm design problem described in Equation 20 was solved using a mixed integer genetic algorithm optimizer [27]. The user defined parameters are summarized in Table 2.

Table 2 User defined inputs and bounds supplied for the swarm design problem.

Parameter	Value
Coverage requirement	85 %
Maximum ground resolution	1 m
Minimum elevation angle	5 deg
Altitude tolerance	5 km
Minimum periapsis altitude	300 km
Maximum #visits	5
Maximum #spacecraft in each visit	5

The genetic algorithm utilized a uniform stochastic sampling scheme with a uniform crossover fraction of 80%. The solution was able to converge to an optimal solution in 22 generations, exploring a total of 2300 designs. The results of the optimization showing the evolution of the mean and best swarm size across different generations of designs, along with the selected optimal solution are presented in Figure 8. As seen in Figure 8, the optimal solution contained a 4 spacecraft swarm, which visits Phobos at two locations using two spacecraft each visit.

D. Operation

The hyperbolic trajectories of the swarm at Mars are presented in Figure 9. All trajectories were found to have the same RAA and DAA as determined from the trajectory design problem. This can also be seen in Figure 9 as both trajectories have nearly parallel incoming trajectories. As seen here, the swarm has two encounters with Phobos. The operation sampled during one of the encounters is presented in Figure 10.

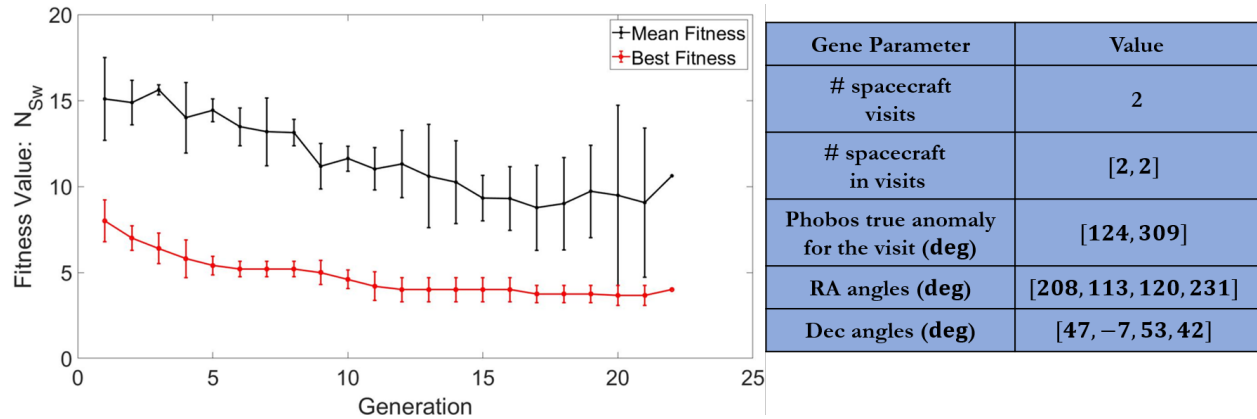


Fig. 8 Progress of the genetic algorithm showing the convergence to an optimal solution (left) along with the selected optimal solution (right).

The swarm is collectively able to cover a total of 86.5% of Phobos' surface as visualized in Figure 11, thus meeting the requirements of the mission objectives.

V. Discussion

The current work described the development of an automated mission design architecture for spacecraft swarm missions. The specific type of mission we addressed here was generating global surface maps of planetary moons through flybys of spacecraft swarms. In doing so, few crucial challenges to developing such architectures were raised. Firstly, we noticed that mission design is a highly multidisciplinary problem. For instance, the design of the spacecraft camera, and the interplanetary trajectory influence the swarm performance. For this reason, having a unifying design tool such as IDEAS can be beneficial over traditional decoupled mission design schemes. More importantly, This work also addresses a major challenge that shows up for designing the swarm flybys, which is to ensure that all trajectories share the same incoming asymptote. It can be noted here that, despite the assumption in the current work that all the spacecraft in the swarm were launched individually, having the same asymptote supports both mother-daughter, and single launch architectures.

The following are a few important contributions of the current work to the state-of-the-art mission design. The

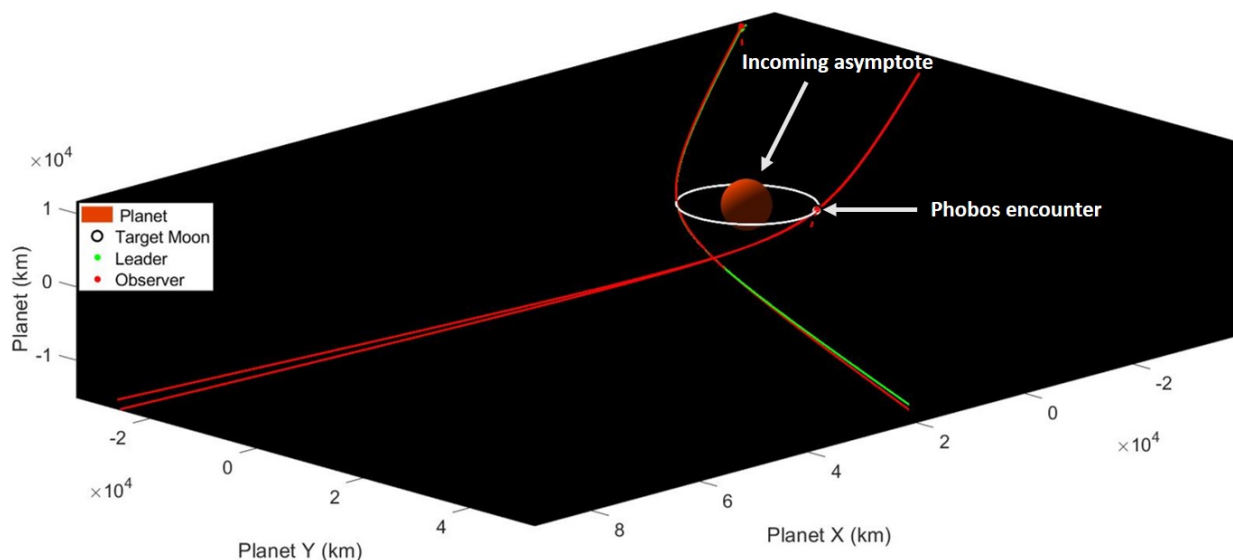


Fig. 9 The hyperbolic trajectories of the swarm showing the arrival asymptote and the encounter locations.

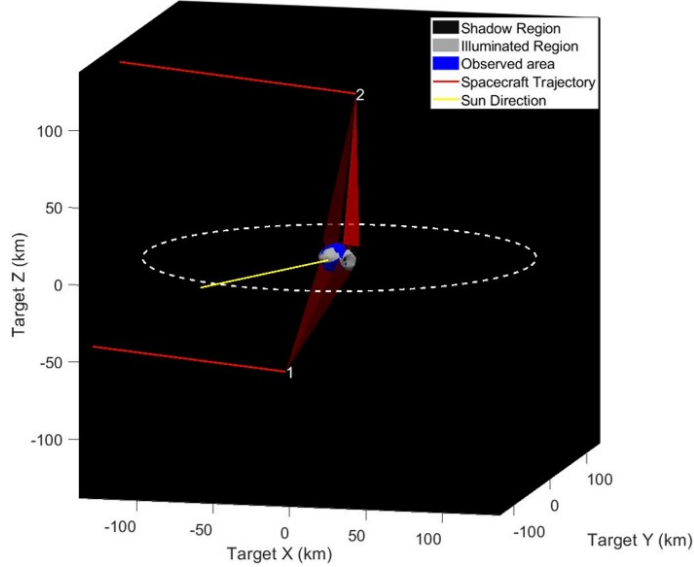


Fig. 10 The flyby mapping operation of the swarm sampled at one of the encounters.

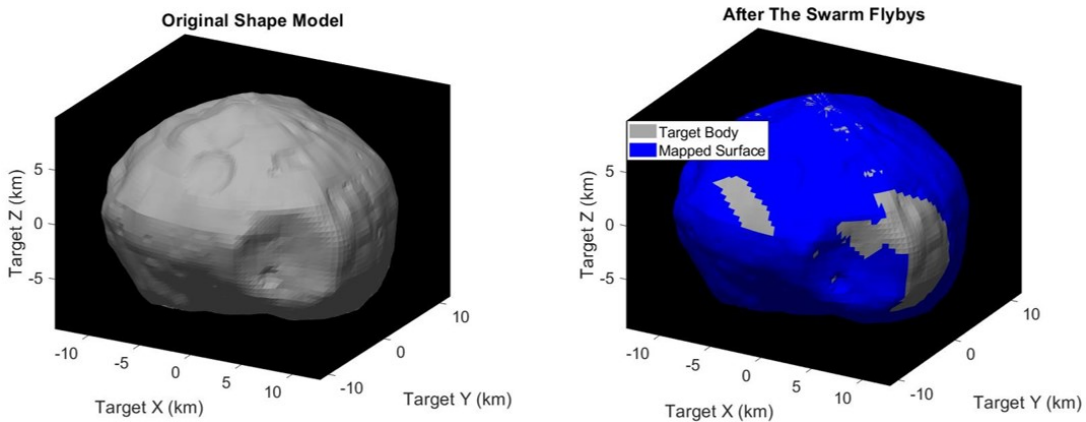


Fig. 11 The shape model of Phobos used to model its surface (left) along with the final coverage after the flybys of the swarm (right).

current work developed novel algorithms to design flyby trajectories where an encounter point and incoming asymptote were specified. Next, we proceeded to show how such trajectories would factor into the design of a small body mapping mission, by developing a unifying mission design scheme. Finally, we applied these schemes to a notional moon mapping mission where the algorithms presented were successfully demonstrated.

VI. Conclusion

This paper presents the development of a new mission architecture capable of automatically designing swarm flyby missions to planetary moons. We further analyze how the design methodology of the IDEAS framework, and its individual modules (spacecraft, swarms, and trajectory) influence the design of the overall mission. We then formulated the individual trajectory, and swarm design as optimization problems. A crucial element of the swarm design problem was to constrain the mapping trajectories of the spacecraft swarm, to share the same arrival asymptote as the designed hyperbolic interplanetary trajectory. To address this problem, we presented a set of nonlinear equations which determined the inertial velocity vector during the encounter with the moon. Finally, the algorithms developed in this work is demonstrated through automated design of a notional swarm mission to map the surface of the Martian moon Phobos. Our future work on IDEAS will focus on incorporating high fidelity dynamical models into the design.

Additionally, perturbations such as launch errors will be factored into the design as well. Such perturbations can be used to estimate the probabilistic correction maneuvers need in real mission, thus making IDEAS a more accurate and realistic mission design framework.

References

- [1] Board, S. S., Council, N. R., et al., *Vision and voyages for planetary science in the decade 2013-2022*, National Academies Press, 2012.
- [2] Castillo-Rogez, J. C., Pavone, M., Nesnas, I. A., and Hoffman, J. A., “Expected science return of spatially-extended in-situ exploration at small solar system bodies,” *IEEE Aerospace Conference*, 2012, pp. 1–15.
- [3] Nallapu, R., Thoesen, A., Garvie, L., Asphaug, E., and Thangavelautham, J., “Optimized Bucket Wheel Design for Asteroid Excavation,” *Proceedings of the International Astronautical Congress, IAC*, International Astronautical Federation, IAF, 2016.
- [4] Geurts, K., Fantinati, C., Ulamec, S., and Willnecker, R., “Rosetta lander: on-comet operations execution and recovery after the unexpected landing,” *14th International Conference on Space Operations*, 2016, p. 2509.
- [5] Scheeres, D. J., *Orbital motion in strongly perturbed environments: applications to asteroid, comet and planetary satellite orbiters*, Springer, 2016.
- [6] Melman, J., Mooij, E., and Noomen, R., “State propagation in an uncertain asteroid gravity field,” *Acta Astronautica*, Vol. 91, 2013, pp. 8–19.
- [7] Fimmel, R. O., Van Allen, J. A., and Burgess, E., *Pioneer: first to Jupiter, Saturn, and beyond*, Vol. 446, Scientific and Technical Information Office, National Aeronautics and Space . . . , 1980.
- [8] Kohlhase, C., and Penzo, P., “Voyager mission description,” *Space science reviews*, Vol. 21, No. 2, 1977, pp. 77–101.
- [9] Nallapu, R., and Thangavelautham, J., “Attitude Control of Spacecraft Swarms for Visual Mapping of Planetary Bodies,” *2019 IEEE Aerospace Conference Proceedings*, IEEE, 2019.
- [10] Simpson, J., Rabinowitz, D., Tuzzolino, A., Ksanfomality, L., and Sagdeev, R., “The dust coma of comet P/Halley: Measurements on the Vega-1 and Vega-2 spacecraft,” *Exploration of Halley’s Comet*, Springer, 1988, pp. 742–752.
- [11] Keller, H., Arpigny, C., Barbieri, C., Bonnet, R., Cazes, S., Coradini, M., Cosmovici, C., Delamere, W., Huebner, W., Hughes, D., et al., “First Halley multicolour camera imaging results from Giotto,” *Nature*, Vol. 321, No. 6067s, 1986, p. 320.
- [12] Hirao, K., and Itoh, T., “The Sakigake/Suisei encounter with comet P/Halley,” *Exploration of Halley’s Comet*, Springer, 1988, pp. 39–46.
- [13] Von Roseninge, T. T., Brandt, J. C., and Farquhar, R. W., “The international cometary explorer mission to comet Giacobini-Zinner,” *Science*, Vol. 232, No. 4748, 1986, pp. 353–356.
- [14] Brownlee, D., “The Stardust mission: analyzing samples from the edge of the solar system,” *Annual Review of Earth and Planetary Sciences*, Vol. 42, 2014, pp. 179–205.
- [15] Buratti, B. J., Britt, D., Soderblom, L., Hicks, M., Boice, D., Brown, R., Meier, R., Nelson, R., Oberst, J., Owen, T., et al., “9969 Braille: Deep Space 1 infrared spectroscopy, geometric albedo, and classification,” *Icarus*, Vol. 167, No. 1, 2004, pp. 129–135.
- [16] Wertz, J. R., Everett, D. F., and Puschell, J. J., *Space mission engineering: the new SMAD*, Microcosm Press, 2011.
- [17] Nallapu, R., and Thangavelautham, J., “Spacecraft Swarm Attitude Control for Small Body Surface Observation,” *2019 Advances in the Astronautical Sciences(AAS)-GNC Conference Proceedings*, AAS-GNC, 2019.
- [18] Nallapu, R., Kalita, H., and Thangavelautham, J., “On-Orbit Meteor Impact Monitoring Using CubeSat Swarms,” *2018 Advanced Maui Optical Science (AMOS) Proceedings*, AMOS Tech., 2018.
- [19] Nallapu, R., and Thangavelautham, J., “Cooperative Multi-spacecraft Observation of Incoming Space Threats,” *2019 Advanced Maui Optical Science (AMOS) Proceedings*, AMOS Tech., 2019.
- [20] Nallapu, R., Vance, L. D., and Thangavelautham, J., “Automated Design Architecture for Lunar Constellations,” *2020 IEEE Aerospace Conference Proceedings*, IEEE, 2020.

- [21] Nallapu, R., and Thangavelautham, J., "Towards End-To-End Design of Spacecraft Swarms for Small-Body Reconnaissance," *Proceedings of the International Astronautical Congress, IAC*, International Astronautical Federation, IAF, 2019.
- [22] Vallado, D., *Fundamentals of Astrodynamics and Applications*, 2007.
- [23] Schaub, H., and Junkins, J. L., *Analytical mechanics of space systems*, American Institute of Aeronautics and Astronautics, 2013.
- [24] "Space Frieger Shape model catalogue," <https://space.frieger.com/asteroids/>, 2013. Accessed: 11-30-2019.
- [25] Pong, C. M., Lim, S., Smith, M. W., Miller, D. W., Villaseñor, J. S., and Seager, S., "Achieving high-precision pointing on ExoplanetSat: initial feasibility analysis," *Space Telescopes and Instrumentation 2010: Optical, Infrared, and Millimeter Wave*, Vol. 7731, International Society for Optics and Photonics, 2010, p. 77311V.
- [26] Russell, R. P., "On the solution to every lambert problem," *Celestial Mechanics and Dynamical Astronomy*, Vol. 131, No. 11, 2019, p. 50.
- [27] Conn, A. R., Gould, N. I., and Toint, P., "A globally convergent augmented Lagrangian algorithm for optimization with general constraints and simple bounds," *SIAM Journal on Numerical Analysis*, Vol. 28, No. 2, 1991, pp. 545–572.